Combined High Resolution UV and Microwave Results: Structure of the Benzonitrile·Water Complex

R. M. Helm, H.-P. Vogel, H. J. Neusser

Institut für Physikalische und Theoretische Chemie, Technische Universität München, Lichtenbergstr. 4, D-85748 Garching

V. Storm, D. Consalvo*, and H. Dreizler

Institut für Physikalische Chemie, Universität Kiel, Ludewig-Meyn-Str. 8, D-24098 Kiel

* Institut für Physikalische Chemie, RWTH Aachen, Templergraben 59, D-52056 Aachen

Z. Naturforsch. **52 a,** 655–664 (1997); received July 29, 1997

High resolution ultraviolet (UV) and molecular beam Fourier transform microwave (MB FTMW) spectroscopy of the benzonitrile·water (BZNW) cluster were performed to measure cluster structures in the S_0 and S_1 states. The MW experiments provide additional information on the structure and the ^{14}N-nuclear quadrupole coupling in the ground state S_0, the UV experiments on the dynamics in S_1.

The rotationally resolved sub-Doppler UV spectra of BZNW were measured by mass-selective resonance-enhanced two-photon ionization. For the first time this UV technique has been applied to hydrogen-bonded clusters. From the UV spectra the rotational constants are obtained by Correlation Automated Rotational Fitting. The MW spectra were analyzed with the model of a centrifugally distorted rotor including nuclear quadrupole coupling. A r_0-fit of the water position within the cluster is performed. The water is found to be located with its oxygen nearly in the plane of benzonitrile (BZN). For S_0 (S_1), the distance of the oxygen to the ortho hydrogen is $r_0 = 2.477(4)$ Å (2.457(2) Å) and the angle to the ortho carbon-hydrogen bond 143.34(2)° (141.91(3)°). The structure differences in S_1 and S_0 can be explained by the structure changes of the BZN molecule. A line broadening, which points to a faster decay in S_1 upon clustering with the polar solvent, is observed for the BZNW cluster.

I. Introduction

The structure of benzonitrile·water ($C_6H_5CN·H_2O$, BNZW) in the electronic ground and excited state has been a matter of current interest [1, 2]. The prototype system of water loosely bound to a cyano group allows the investigation of the fundamental properties of a hydrogen bonding between water and aromatic molecules. Our research is not only motivated by the recent experimental results on the clustering of benzonitrile (BZN) [1 - 5], benzene and related molecules [6 - 8], but also by the theoretical prediction of a twisted internal charge transfer reaction (TICT) [9, 10] in BZN. The charge transfer is expected to be influenced by the solvent [11, 12] and has been the subject of recent experiments with lower resolution for the related aminobenzonitriles [13 - 15].

Reprint requests to Prof. H. J. Neusser, Fax: +49 89 289-13412 or Prof. H. Dreizler, Fax: +49 431 880-1416/1704.

The bonding distance is expected to affirm the character of the bonding. The main contribution is from hydrogen bonding, but due to the large permanent dipole moment of BZN of 4.18 debye [16] an influence of the dipole-dipole interaction on the bonding is expected different from the hydrogen bonding recently investigated in phenol·water [6] and pyridone·water [8].

The combination of results from the MW and mass-resolved UV experiments with rotational resolution joins the virtues of the two techniques and is shown to result in a successful structure determination. High resolution resonance enhanced two-photon experiments can resolve the rotational structure of a vibronic transition for a species with defined mass within all clusters present in the molecular beam. By fitting the data some predictions about the structure can be made. The gained predictions are not exact, but they can be used as approximate input for MW experiments, so that the search and assignment of rotational transitions is possible and leads to accurate ground state

0932-0784 / 97 / 0800-0655 $ 06.00

rotational constants. These results allow the exact interpretation of the UV experiments leading to detailed information about the S_1 electronically excited state.

II. Experimental

A) Microwave Experiments

The microwave experiments were performed in Kiel using molecular beam (MB) Fourier transform microwave (FTMW) spectrometers with a resonator operating in the TE_{01} (H_{01}) mode of a cylindrical cavity in the range 1 to 4 GHz [17] and a Fabry-Perot resonator operating from 7 to 26.5 GHz [18]. BZN, C_6H_5CN, supplied by Fa. Aldrich, Steinheim, was kept upstream the beam nozzle in a small vessel. The surface of the liquid substance was exposed to a stream of argon or preferably helium containing about 0.5 % of water vapour. A sample of 70 % enriched $H_2^{18}O$, which was used to gain more information about the structure was supplied by Cambridge Isotope Laboratories. A backing pressure of 120 kPa was used. Additional measurements in the region between 4 and 8 GHz were performed in Aachen, with a MB FTMW spectrometer described in [19]. First the spectrometers were used in the scan mode, see [19], to locate the transitions. These were afterwards recorded in the high resolution mode with 8 K sample points at a sample distance of 10 ns or 40 ns. From 0.5 to 16 K measuring cycles were necessary to obtain a good signal to noise ratio.

B) UV Experiments

The UV experiments were performed in Munich. For the measurements, 5 bar backing pressure of Ar and 10 mbar of water were expanded supersonically through a specially developed heated (60 ^{0}C) reservoir of fluid BZN just in front of a pulsed valve (modified Bosch) with a 200 µm orifice. The experimental apparatus for the recording of high resolution UV spectra by mass-selected resonance-enhanced two-photon ionization was described in detail in our previous work [20]. Briefly, the light of an Ar^+-laser (Spectra Physics 171) pumps a cw single-mode ring dye laser (Coherent CR 699/29, Rhodamine 110). Its output is pulsed amplified in three XeCl excimer laser (Lambda Physik MSC 201) pumped amplifier stages operating with the dye Coumarine 307 [21]. After frequency doubling, the UV pulses have a duration of 10 ns (FWHM). In the present experiment the pulse energy was reduced by transmission filters to 0.2 mJ. The frequency width of the laser light is 70 MHz (FWHM), which is close to the Fourier transform limit. For the second photon absorption step leading to ionization the light of a commercial XeCl excimer laser-pumped broad band dye laser (Lambda-Physik FL 2002, Coumarin 102) is frequency doubled and directed perpendicularly to the molecular beam counterpropagating to the excitation laser beam. The light pulses of the ionization laser have an energy of 0.2 mJ and a duration of 10 ns.

The mass selective detection of the produced ions is realized by a home-built linear time of flight mass spectrometer. A gated boxcar integrator (Stanford Research Systems SR250) integrates the signal of the channel plates in the appropriate time window, a microcomputer (Force CPU-37) controls the laser frequency and records the signal intensity and the calibration signals.

Simultaneously recorded were the calibration signals with fractions of the visible cw laser light. The relative frequency calibration signal is provided by a 150 MHz Fabry-Perot interferometer transmission spectrum, and the absolute frequency calibration signal by an iodine vapor fluorescence excitation spectrum, which is positioned according to [22, 23].

III. Results and Discussion

The shape of the UV spectrum, which is described in detail below, provides a first qualitative estimate of the structure. The orientation of the dipole transition moment with respect to the principal axes of the cluster makes up the shape of the spectrum due to the specific selection rules. The selection rules can be stated by means of K_a and K_c, the quantum numbers of rotation about the a and c axes in the limiting cases of the corresponding prolate and oblate symmetric tops. If the transition moment is oriented parallel to the a-axis the selection rules $\Delta K_a = 0, \pm 2, \ldots$ and $\Delta K_c = \pm 1, \pm 3, \ldots$ apply. For a position parallel to the b-axis $\Delta K_a = \pm 1, \pm 3, \ldots$ and $\Delta K_c = \pm 1, \pm 3, \ldots$, for a position parallel to the c-axis $\Delta K_a = \pm 1, \pm 3, \ldots$ and $\Delta K_c = 0, \pm 2, \ldots$ apply. For any other position of the transition moment contributions from the three projections on the principal axes determine the relative intensities of the transitions [24]. For pure a- or b-type transitions the spectrum will consist of two broad wings with basically a hole in the middle. On the other hand if the transition moment is oriented parallel to the c-axis

the spectrum would consist of two broad wings and a sharp central peak outranging the side wings.

For the BZN monomer the orientation of the transition moment parallel to the b-axis is known [3]. As is known from high resolution spectroscopy of other clusters, the orientation of the transition moment is only slightly affected by clustering, but the direction of the main axes of the moment of inertia tensor is changed. Therefore a position of the water above the ring would change the spectrum to c-type and the b-axis of the BZN monomer would become the c-axis of the cluster like in the case of BZN·Ar [3]. On the other hand, a position of the water in the plane of BZN would only turn the b-axis of the monomer within the a-b-plane and a mixed a- and b-type spectrum is expected.

The latter is indeed the kind of spectrum we observe, and therefore the oxygen of the water must be located near the BZN plane in contrast to benzene·water [25] or BZN·Ar [3, 4], where the water or argon, respectively, is positioned above the ring. This can be concluded from the highly resolved UV spectrum without a detailed analysis of its rotational structure. This is the starting point for the MW experiment.

A) Analysis of the Microwave Spectra

The data from the initial UV experiments provided starting values for the rotational constants in a range of about 150 MHz maximum within the final constants. After scans [26] covering regions of about some 100 MHz transitions of the BZNW cluster could be identified. It was of great help, that the BZN rotational spectrum was thoroughly investigated (Table 3 of [4], [27]). The cluster lines assignment was verified by an analysis with the model of a centrifugally distorted asymmetric rotor [28] using the program ZFAP4 [29]. In addition the ^{14}N-hyperfine structure (hfs) could be analyzed with high accuracy [30]. The program HFS [31, 32] was used in order to confirm the assignment. Following this procedure two isotopomers, C_6H_5CN-$H_2^{16}O$ and C_6H_5CN-$H_2^{18}O$, were studied. The lines are given in Table 1 and Table 2 and the resulting rotational, centrifugal distortion, and quadrupole coupling constants are listed in Table 3. It is intended to investigate further isotopomers. In Fig. 1 a typical recording of an observed rotational transition is displayed. It should be mentioned that the a–type rotational spectrum of BZN is modified to an a– and b–type spectrum of the cluster, as the permanent dipole moment

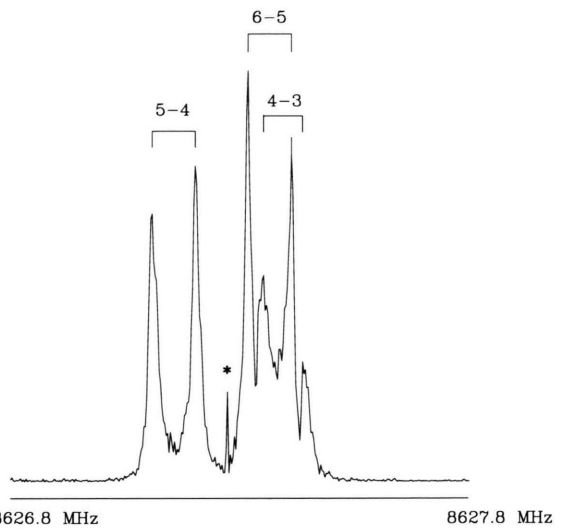

Fig. 1. Rotational transition $J_{K_a K_c} = 5_{24} - 4_{23}$ of BZNW showing ^{14}N–hfs. 16 K data points were recorded with a sample interval of 40 ns and 6 K averaging cycles. As carrier gas He, saturated with H_2O, has been used. Backing pressure 120 kPa. The star (*) indicates a coherent perturbation at the polarisation frequency of 8627.27 MHz.

of BZN is differently oriented in the principal inertia axis system of the cluster. This allows the determination of all rotational constants of the ground state S_0 with roughly the same precision. Unfortunately this precision can usually not be transferred to the structure. In the case of weakly bound complexes the problem is further complicated by the occurrence of large amplitude motions.

B) Analysis of the UV Spectra

From the different cluster species present in the experiment only the ion current at the mass of 121 u, i. e. the mass of BZNW, is selected. In Fig. 2 the ion signal is plotted against the laser frequency between 36442.25 cm^{-1} and 36444.0 cm^{-1}. The ionization laser wavelength was fixed at 470 nm. The measured spectrum of the vibrationless $S_1 \leftarrow S_0$ transition has two broad wings with a hole in the center, as is typical for a- and b-type transitions with a P- and R-branch and missing Q-branch, as discussed qualitatively above.

To determine the rotational constants we performed a fit of the measured spectrum to the rigid asymmetric rotor dipole transition [33] using the method of Correlation Automated Rotational Fitting (CARF) [3]. The technique determines the crosscorrelation between

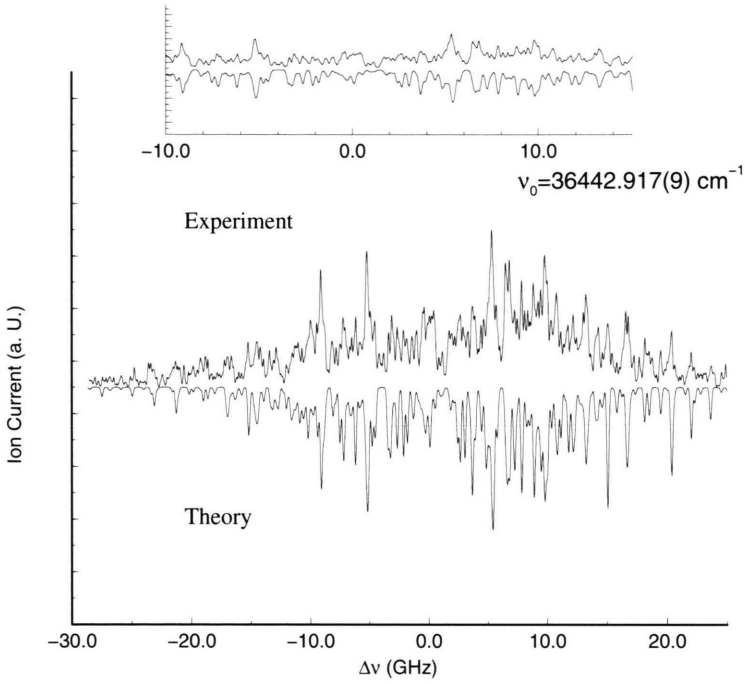

Fig. 2. Highly resolved UV spectrum of BZNW: $S_1 \leftarrow S_0,0_0^0$ transition. Upright traces: experimental spectrum. Inverted traces: calculated spectrum using the rotational constants found in this work by Correlation Automated Rotational Fitting. Top: magnified central part of the spectrum.

Table 1. Observed rotational MW transitions of BZNW (^{16}O).

$J'_{K'_a K'_c}$ -$J_{K_a K_c}$	F'-F	obs. [MHz]	obs.–calc. [kHz]	$J'_{K'_a K'_c}$ -$J_{K_a K_c}$	F'-F	obs. [MHz]	obs.–calc. [kHz]	$J'_{K'_a K'_c}$ -$J_{K_a K_c}$	F'-F	obs. [MHz]	obs.–calc. [kHz]
1_{01}-0_{00}	0-1	1737.6768	–0.3	4_{13}-3_{12}	3-2	7402.3240	1.9	6_{33}-5_{32}	5-4	10590.9892	–0.4
	1-1	1735.4873	–0.6		4-3	7402.2281	–1.0		6-5	10590.6932	0.4
	2-1	1736.3642	0.8		5-4	7402.3462	–1.7		7-6	10590.9491	–0.3
2_{12}-1_{11}	1-0	3218.2096	–5.6	5_{05}-4_{04}	4-3	8251.4835	–1.0	7_{07}-6_{06}	6-5	11199.3575	–4.6
	1-1	3217.3996	–6.8		5-4	8251.4948	–1.0		8-7	11199.3849	–0.5
	2-1	3216.4832	–2.8		6-5	8251.5368	4.2	8_{18}-7_{17}	8-7	12534.3060	–0.3
2_{02}-1_{01}	1-0	3447.5268	1.5	5_{15}-4_{14}	5-4	7951.1171	3.2		7-6	12534.3171	2.5
	1-1	3449.7169	2.4		6-5	7951.1853	0.5		9-8	12534.3328	0.6
	2-2	3447.3633	–0.7	5_{23}-4_{22}	4-3	9056.2556	–1.6	7_{16}-6_{15}	6-5	12640.3832	–2.2
	3-2	3448.3129	0.9		5-4	9056.0449	–1.9		7-6	12640.3569	–5.1
2_{11}-1_{10}	1-0	3728.8425	5.1		6-5	9056.2324	–5.0		8-7	12640.4046	4.0
	2-1	3726.9211	3.2	5_{24}-4_{23}	4-3	8627.3872	–1.0	7_{25}-6_{24}	6-5	12913.4950	–0.8
	3-2	3727.8213	4.9		5-4	8627.1526	–1.6		7-6	12913.4367	1.1
3_{13}-2_{12}	3-2	4811.1700	0.5		6-5	8627.3656	–0.8	7_{25}-6_{24}	8-7	12913.5048	2.5
	4-3	4811.4389	1.2	5_{32}-4_{31}	4-3	8779.9787	–1.4	9_{09}-8_{08}	8-7	14112.9428	1.6
3_{22}-2_{21}	2-1	5209.3749	0.2		5-4	8779.4263	–1.1		9-8	14112.9351	–0.3
	3-2	5207.9154	0.2		6-5	8779.8693	–1.5		10-9	14112.9569	1.5
	4-3	5208.8559	2.6	5_{33}-4_{32}	4-3	8750.3047	–2.2	8_{17}-7_{16}	7-6	14262.0160	–0.5
3_{12}-2_{11}	2-1	5575.6426	–3.2		5-4	8749.7466	–4.5		8-7	14261.9933	–1.0
	3-2	5575.3629	–4.0		6-5	8750.1960	–1.1		9-8	14262.0293	1.0
	4-3	5575.6243	–2.1	6_{06}-5_{05}	5-4	9738.2494	0.2	1_{11}-0_{00}	0-1	3622.2448	–1.6
4_{14}-3_{13}	3-2	6390.0616	0.3		7-6	9738.2842	3.0		1-1	3623.0525	–2.7
	4-3	6389.9856	–0.4	6_{16}-5_{15}	5-4	9494.3880	0.1		2-1	3622.7316	–0.1
	5-4	6390.1101	0.7		6-5	9494.3693	–0.8	2_{12}-1_{01}	1-0	5102.7873	2.8
4_{23}-3_{22}	3-2	6926.1923	0.1		7-6	9494.4178	1.0		2-1	5104.0508	–2.5
	4-3	6925.6901	1.2	6_{24}-5_{23}	5-4	10985.3177	–0.5		3-2	5103.7746	5.5
	5-4	6926.0917	2.3		6-5	10985.2125	0.7	8_{08}-7_{17}	7-6	12348.0838	–6.6
4_{22}-3_{21}	3-2	7155.8747	0.8	6_{25}-5_{24}	6-5	10308.9217	3.8		9-8	12348.1123	4.4
	4-3	7155.3954	2.8		7-6	10309.0450	–1.5	8_{18}-7_{07}	7-6	12840.5584	–6.6
	5-4	7155.7769	3.2	6_{34}-5_{33}	5-4	10513.7101	2.0		9-8	12840.5859	3.0
					6-5	10513.4126	6.6	6_{25}-5_{14}	5-4	14555.2054	–7.2
					7-6	10513.6685	1.3		6-5	14555.3056	2.7
									7-6	14555.2539	4.5

Table 2. Observed rotational MW transitions of BZNW (^{18}O).

$J'_{K'_aK'_c}$ -$J_{K_aK_c}$	F'-F	obs. [MHz]	obs.–calc. [kHz]	$J'_{K'_aK'_c}$ -$J_{K_aK_c}$	F'-F	obs. [MHz]	obs.–calc. [kHz]	$J'_{K'_aK'_c}$ -$J_{K_aK_c}$	F'-F	obs. [MHz]	obs.–calc. [kHz]
1_{01}-0_{00}	0-1	1673.6900	1.8	6_{16}-5_{15}	5-4	9164.3238	3.8	9_{09}-8_{08}	9-8	13635.6381	–3.2
	1-1	1671.5936	–1.9		6-5	9164.2980	–3.5		10-9	13635.6688	4.8
	2-1	1672.4345	2.0		7-6	9164.3529	4.4	1_{11}-0_{00}	0-1	3539.8590	0.1
2_{12}-1_{11}	1-0	3103.7490	–3.0	6_{06}-5_{05}	6-5	9407.7618	0.9		1-1	3540.5615	0.0
	2-1	3102.1168	–6.1		7-6	9407.7939	–5.1		2-1	3540.2844	3.5
	3-2	3102.9976	–1.8	6_{25}-5_{24}	6-5	9935.1665	–2.9	5_{15}-4_{04}	4-3	8717.9225	–4.3
2_{02}-1_{01}	1-0	3321.9131	1.0		7-6	9935.2953	1.2		5-4	8717.9414	3.3
	1-1	3323.9972	–7.6	6_{24}-5_{23}	6-5	10558.8163	2.8		6-5	8717.9742	0.6
	2-2	3321.7520	–0.4		7-6	10558.9115	0.4	3_{22}-2_{11}	2-1	10620.6903	0.2
	2-1	3322.5946	5.2	7_{17}-6_{16}	6-5	10640.1714	–1.8		3-2	10621.1614	3.2
	3-2	3322.6620	–0.1		7-6	10640.1623	1.8		4-3	10620.8590	1.6
2_{11}-1_{10}	1-0	3587.5120	5.7		8-7	10640.1986	3.5	8_{08}-7_{17}	8-7	11901.6691	–2.3
	2-1	3585.6492	1.7	7_{16}-6_{15}	6-5	12185.5701	–2.6		9-8	11901.7002	4.9
	3-2	3586.5059	1.5		7-6	12185.5418	–2.5	8_{18}-7_{07}	7-6	12428.4536	–1.2
5_{05}-4_{04}	5-4	7967.6944	–1.8		8-7	12185.5898	3.9		8-7	12428.4370	–4.1
	6-5	7967.7407	1.9	8_{08}-7_{07}	7-6	12227.2706	–0.2		9-8	12428.4742	2.6
5_{24}-4_{23}	4-3	8312.6551	6.4		8-7	12227.2586	–1.9	4_{22}-3_{13}	3-2	13695.1220	2.1
	5-4	8312.4251	1.6		9-8	12227.2887	0.7		4-3	13695.8621	–2.4
	6-5	8312.6262	–1.5	9_{19}-8_{18}	9-8	13555.1285	1.1		5-4	13695.3307	–4.7
5_{14}-4_{13}	4-3	8855.8733	–8.6		10-9	13555.1535	4.3				
	5-4	8855.8381	3.6								
	6-5	8855.9035	0.1								

Table 3. Experimental rotational, van Eijck [44] centrifugal distortion, and quadrupole coupling constants of the BZNW complex. Moments of inertia I_g, inertia defect Δ, and planar moments P_g (conversion factor 5.05376 · 10^5 MHz amu Å^2 [39]), κ Ray-asymmetry parameter, N number of hyperfine components, σ standard deviation.

	$H_2^{16}O$ (S_0)	$H_2^{18}O$ (S_0)	$H_2^{16}O$ (S_1)
A/MHz	2882.2886(22)	2825.0638(44)	2821.6(23)
B/MHz	995.71865(39)	957.02927(41)	984.3(14)
C/MHz	740.49971(23)	715.26447(24)	729.0(33)
κ	–0.7617	–0.7706	–0.756(3)
D'_J/kHz	0.2576(15)	0.2598(25)	
D'_{JK}/kHz	–0.678(16)	–0.763(57)	
D'_K/kHz	4.21(45)	4.54(80)	
δ'_J/kHz	0.0874(16)	0.0861(20)	
R'_6/kHz	–0.0097(11)	–0.0092(22)	
χ_{aa}/MHz	–2.9196(29)	–2.7904(33)	
χ_{bb}/MHz	1.0824(53)	0.936(13)	
χ_{cc}/MHz	1.8372(53)	1.854(13)	
σ/kHz	3.2	3.6	CARF
N	69	58	CARF
I_a/amu Å^2	175.338	178.890	179.1(2)
I_b/amu Å^2	507.549	528.068	513.4(7)
I_c/amu Å^2	682.480	706.559	693.2(31)
P_a/amu Å^2	507.346	527.869	513.8(16)
P_b/amu Å^2	175.135	178.691	179.4(16)
P_c/amu Å^2	0.219	0.200	–0.4(16)
Δ/amu Å^2	–0.407	–0.399	0.7(32)
Origin/cm^{-1}			36442.917(9)

experiment and simulation. The position of the cross-correlation peak defines the relative position of experimental and simulated spectrum and therefore the origin of the transition. The height of the crosscorrelation peak is a criterion for the quality of the simulation and is adapted sequentially in a fit procedure. This is the first demonstration of this technique for complex spectra. The S_0 rotational constants were taken from the MW experiments in the previous section and not changed during the fit. The fit was started with the ground state values for both electronic states and relative intensities of a- and b-type transitions of 30 to 70. After the exact microwave data was available we assumed that the orientation change of the transition moment upon clustering is negligible and therefore the new orientation of the BZN monomer b-axis, which can be found from the orthogonal transformation matrix in Table 6, defines the orientation of the transition moment in the cluster. This means an intensity ratio of a- to b-type of 19 to 81 and an orientation of the transition moment of 26° with respect to the principal b-axis of the cluster.

In Table 3 the rotational constants resulting from the fit are given together with the MW data. The error of the rotational constants is given by the standard deviation of the fits of 12 separately measured experimental spectra of the band and additionally it is ensured that the visual agreement between experimental and theoretical spectrum decreases noticeably when leaving the error bars. In the lower inverted trace of Fig. 2 the spectrum calculated for a rotational temperature of 1.0 K with the constants of Table 3 is shown representing the best agreement with the measured spectrum. The agreement of line positions

Table 4. UV linewidth of BZN monomer for several clustering partners.

Molecule/Cluster	Linewidth [MHz]
C_6H_5CN	<100[a]
$C_6H_5CN{\cdot}Ar$	150[a]
$C_6H_5CN{\cdot}H_2O$	180[b]
$C_6H_5CN{\cdot}(H_2O)_2$	unresolved[c]

[a] [3]; [b] this work; [c] [34].

in the central part of the spectrum is demonstrated in the inset of Fig. 2 with a magnified part of the spectrum. A further fit of intensities which could include a two temperature model, saturation, intensity dependent noise, constant ground noise and different dipole transition moment orientations could result in a better optical agreement of theory and experiment in Fig. 2 but would not change the accuracy of the inertial constants. This has been verified in a series of fits performed in addition to the one shown in Figure 2.

For the presentation the calculated stick spectrum was convoluted with a Gaussian line shape of 180 MHz (FWHM) to match the resolution in the experimental spectrum. The observed linewidth of 180 MHz is larger than expected from the experimental resolution. An increasing line broadening is observed for a series of spectra: for unchanged experimental conditions we observed a linewidth of the BZN monomer of less than 100 MHz (instrumental resolution), a linewidth of the BZN·Ar complex of 150 MHz [3] and in this work of the BZNW of 180 MHz. Furthermore, measurements of the $BZN{\cdot}(H_2O)_2$ cluster [34] show an unresolved rotational structure. The lifetimes are summarized in Table 4. There are several possible explanations for these results: Line broadening due to saturation, to unresolved line splitting or to fast decay dynamics. Since the expansion conditions were not changed in the series of the experiments and the laser intensity was optimized for highest spectral resolution, saturation as a source of the broadening seems to be unlikely. A line splitting due to the torsional motion of the water moiety may be below the experimental resolution and thus could lead to a broadening of the observed linewidth. This, however, would not explain the line broadening observed in BZN·Ar. Therefore the most reasonably explanation for the observed line broadening is a decreasing lifetime with increasing cluster size and/or polarity of the solvent. The lifetime of the electronically excited S_1 state decreases with the number and/or the dipole moment of the clustering partners. Ultra short time-resolved and highly resolved dispersed fluorescence experiments may clarify whether the excited electronic states in these species decay to the electronic ground state, to the proposed charge transfer state [11, 12] or whether a fragmentation of the clusters occurs.

Comparing these results for the dynamics with other aromatic water clusters like phenol·water we found that BZNW decays faster upon clustering, whereas phenol·water has a longer lifetime than pure phenol [6]. This may be due to the different nonradiative processes responsible for the dynamics in the two systems.

C) Cluster Structure

First the analysis of the MW data is reported. We assumed in all structural calculations in the S_0 state that the structure of BZN [4, 35] and water [36] is invariant under complexation. Despite of its approximate character this assumption has proved to be a reasonable one for the vibronic ground state if one is mainly interested in the determination of intermolecular structural parameters [37]. However, we think that internal structural changes are expected to be smaller than e. g. in phenol·water or pyridone·water [23, 8] since the bonding is weaker and the bond length is longer in BZNW.

The numbering of the atoms is given in Figure 3. The planar moment P_c or the inertial defect [38] indicates that the cluster is nearly planar. Assuming near planarity for the cluster the number of independent rotational constants is practically reduced to four. Taking O is situated nearly in the BZN plane the main contribution to the inertial defect comes from the water hydrogens. In a r_0 calculation (program ru111 [39, 40]) we fitted the six moments of inertia by varying two in plane parameters i) the "bond" distance r, H_2-O and ii) the angle β, (C_2,H_2,O); additional parameters were also fitted which change the out of plane positions of the water hydrogens in order to account for the experimentally determined inertial defect. The fitting of out of plane parameters will be described in more detail in the following.

In a first calculation the inclination γ of the symmetry axis of water with respect to the BZN plane was additionally fitted (see Fig. 3 for illustration). The atoms H_a and H_b move above (below) and O below (above) the (a,b)-plane of the complex whereas the

Table 5. Structure parameters of the cluster obtained with an r_0–fit. For definition of β and γ see text and Figure 3. Derived parameters below the first line. $\overline{\Delta I_g} = I_{g_{exp}} - I_{g_{calc}}$, $g = a, b, c$ in S_0 mean value for the ^{16}O and ^{18}O isotopomers.

	S_0 (MW)	S_1 (UV)
$r(H_2\text{-}O))$[Å]	2.477(4)	2.457(2)
β ($\angle(C_2, H_2, O)$) [°]	143.34(2)	141.91(3)
γ[°]	33.7(60)	0
r(CM(B)–CM(W)) [Å]	4.152(3)	4.155
$r(H_a - N)$[Å]	2.612(16)	2.631
$\overline{\lvert\Delta I_a\rvert}$[amu Å^2]	0.0017	0.05
$\overline{\lvert\Delta I_b\rvert}$[amu Å^2]	0.0002	0.90
$\overline{\lvert\Delta I_c\rvert}$[amu Å^2]	0.007	0.64

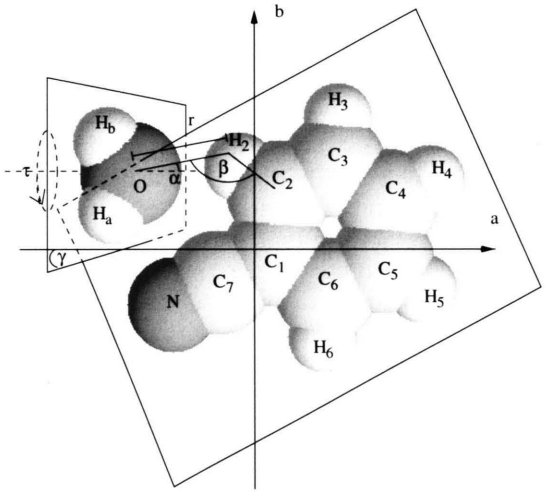

Fig. 3. Experimentally obtained structure of the BZNW complex. Numbering and geometric parameters, see text. Only the structure with the torsion angle $\tau = 0$ is shown. γ describes the inclination of the water plane with respect to the BZN plane.

center of mass of H_2O stays in the plane. The results are given in Table 5. A significant torsion angle τ about the water symmetry axis could not be determined in this calculation. The fitting procedure showed an oscillating behavior around zero.

In Table 6 we give the coordinates of the atoms in the principal axis system of the cluster for $\tau = 0$. The adjustment of the parameters r, β, γ exhausts the information of the six moments of inertia in this calculation.

In a second calculation we tried to adjust r, β, τ and the angle α between the water symmetry axis and the H_2-O direction, see Figure 3. These parameters could be determined, but the resulting ΔI_g were by an order of magnitude worse.

Table 6. Top: cartesian coordinates a_0, b_0, c_0 of the atoms of the ^{16}O BZNW complex in its principal axes system. They resulted from an r_0 fit of the moments of inertia of the ^{16}O and the ^{18}O isotopomers with the r_0–structure of BZN S_0 [27, 35] and S_1 [3] and the assumed structure of water [36]. CM(B) and CM(W) center of mass of BZN and water, respectively. Uncertainty of the last digit is given in parantheses, these errors do not include the errors of the method. Middle: orthogonal transformation matrix between the principal axis systems of BZN and the complex. Bottom: r_s–coordinates a_s, b_s, c_s of O in S_0 for comparison, error estimate according to [45]. UV data based on modeling calculation of [3].

Atom (No)	S_0 a_0[Å]	b_0[Å]	c_0[Å]	S_1 a[Å]	b[Å]	c[Å]
N	−2.2514(1)	−1.6136(3)	0.0082(13)	−2.28	−1.61	0
C_1	0.0854(0)	−0.4737(1)	0.0027(4)	0.05	−0.49	0
C_2	0.1688(1)	0.9218(1)	0.0092(13)	0.15	0.94	0
C_3	1.4254(2)	1.5274(0)	0.0062(9)	1.44	1.56	0
C_4	2.5912(1)	0.7486(1)	−0.0033(6)	2.62	0.75	0
C_5	2.4873(0)	−0.6496(1)	−0.0097(15)	2.52	−0.68	0
C_6	1.2364(1)	−1.2671(0)	−0.0068(10)	1.23	−1.30	0
C_7	−1.2124(1)	−1.1068(2)	0.0057(9)	−1.23	−1.10	0
H_2	−0.7365(2)	1.5126(2)	0.0165(24)	−0.74	1.54	0
H_3	1.5018(3)	2.6057(0)	0.0113(16)	1.52	2.63	0
H_4	3.5619(1)	1.2220(2)	−0.0055(10)	3.60	1.22	0
H_5	3.3841(1)	−1.2532(2)	−0.0171(26)	3.41	−1.28	0
H_6	1.1448(2)	−2.3442(0)	−0.0118(18)	1.15	−2.37	0
O	−3.2090(36)	1.3598(7)	0.0276(42)	−3.20	1.38	0
H_a	−3.653(28)	0.5681(20)	−0.301(44)	−3.73	0.58	0
H_b	−3.747(28)	2.094(19)	−0.293(43)	−3.83	2.09	0
CM (B)	0.5705(0)	−0.2371(1)	0.0015(2)	0.57	−0.24	0
CM (W)	−3.2636(3)	1.3567(5)	−0.0085(12)	−3.26	1.37	0
Transformation matrix	$\begin{pmatrix} 0.899121 & 0.437690 & 0.002880 \\ -0.437632 & 0.899078 & -0.116949 \\ -0.007708 & 0.009255 & 0.999928 \end{pmatrix}$			$\begin{pmatrix} 0.901 & 0.435 & 0 \\ -0.435 & 0.901 & 0 \\ 0 & 0 & 1 \end{pmatrix}$		
Atom (No)	$\lvert a_s\rvert$[Å]	$\lvert b_s\rvert$[Å]	$\lvert c_s\rvert$[Å]			
O (14)	3.2092(2)	1.3839(4)	imaginary			

In a third calculation we adjusted r and β, kept the O–H_a bond directed towards N in the plane and rotated the O–H_b bond about the O–H_a bond out of the plane. The angle $\alpha' = \angle(H_2, O, H_a)$, i.e. the angular position of the water subunit, was also adjusted. In this case a fit of the moments of inertia can be obtained with a quality similar to that reported in Table 5, now with one hydrogen elevated 0.435 Å out of the a,b–plane and $\alpha' = 108.51°$.

These calculations show that the position and orientation of water can be changed and the moments of inertia are still reproduced reasonably. But they also confirm that the information provided by the six moments of inertia is not sufficient to fix the six structural

parameters necessary to describe the position and orientation of water unequivocally.

As the moments of inertia depend on the squares of the coordinates, other geometries cannot in fact be excluded. A possible near planar structure has the oxygen O approaching 1.1 Å to the meta hydrogen H_3. This is an unlikely structure for intracluster bonds.

As the ^{16}O- and ^{18}O-isotopomers were investigated the position of the O atom in the principal axis system of the ^{16}O-isotopomer can be calculated by the r_s method [41]. The r_s coordinates are given at the end of Table 6. The coordinates a_s and b_s agree resonably with the r_0 values and c_s results imaginary, which indicates a substitution near to the (a,b)-inertia plane.

The problem of the structure determination is not completely solved, yet. We are investigating the ^{15}N–BZNW isotopomers to get unequivocal information.

We observed further some *b*–type transitions showing narrow splittings in the order of several 10 kHz. This may indicate a torsional motion, this effect needs further detailed investigations. In Table 1 and 2 the frequencies of split lines are given by the arithmetic mean of the component frequencies.

The ^{14}N nuclear quadrupole coupling [30] may give some information on the complex structure. If the quadrupole coupling tensor of BZN χ_{aa} = −4.2391(18) MHz, χ_{bb} = 2.2893(32) MHz, χ_{cc} = 1.9498(32) MHz [35] is transformed to the principal inertia system of the cluster determined by the r_0 calculation, using the orthogonal matrix given in Table 6, one gets χ'_{aa} = −2.9884 MHz, χ'_{bb} = 1.0384 MHz, χ'_{cc} = 1.9495 MHz. These values differ from the χ_{gg} of Table 3, as the N-H_a "bond" may influence the electronic surrounding of N. The χ'_{gg} may not be used as an argument against near planarity of the complex. The nuclear quadrupole coupling constants χ_{gg} do not exclude a second configuration, as mentioned above, since the angle between the C_2 axis of BZN and the a inertia axis is close to that one of the first configuration.

The UV data is interpreted in a similar way: The inertial tensor of the complex is calculated by transforming the inertial tensor of the water molecule [36] to a representation in the S_1 BZN center of mass coordinate representation [3] and by summation according Steiner's law [42]. We performed a calculation of the rotational constants for different cluster structures and compared them with rotational constants obtained from the experimental data in a fit procedure of the cluster structure using a conjugate gradient algorithm [43]. Since only the relative positioning of the two centers of mass results in a relevant change of the inertial tensor, different fits were performed for τ = 0° and τ = 90°. α was fixed so that the water symmetry axis was orientated towards the hydrogen in ortho position H_2 (hereafter called ortho hydrogen) and γ was set to 0°. The fit quality and the agreement of the inertial defect are much better for the in-plane configuration (τ = 0°), but both configurations converge within the experimental error bar. For determination of the detailed localization of the water molecule in S_1 further isotope substituted measurements are desirable. To visualize the structural results of the fit we calculated the distances relative to the known position of the ortho hydrogen in S_1 [3]. These are summarized in Table 5 and Figure 3. The complete result of the fit is given in Table 6.

The bond length of r_0 = 2.477(4) Å is between the typical bond length of a van der Waals bonded (e. g. van der Waals bond length of BZN·Ar in S_0 (S_1): 3.598 Å (3.52 Å) [3, 4]) and a hydrogen-bonded system (e. g. phenol·water: the distance from the phenol's hydrogen to the water's oxygen in S_0 (S_1) is roughly 1.97 Å (1.93 Å) [6]). The two links of the water to the ortho hydrogen and the C-N group should be compared to recent findings in pyridone·water. In BZNW the distance of the water oxygen to the BZN ortho hydrogen in S_0 (S_1) is 2.477 Å (2.46 Å), whereas the distance between the water hydrogen and the BZN nitrogen is 2.612 Å (2.63 Å). The respective distances in pyridone·water derived from the Kraitchman equations are smaller and increase upon electronic excitation: The distance of the water oxygen to the nearest pyridone hydrogen is 2.01 Å (2.05 Å), the water hydrogen is 1.97 Å (2.05 Å) apart from the pyridone oxygen [8]. This might be due to the different position of the H_2O molecule in the two systems, with the nested character of the water position in BZNW and the side-on position in pyridone·water.

This shows that the bonding in the BZNW complex has hydrogen as well as van der Waals character. The calculation also shows that there are minor structure changes between S_0 and S_1 concerning the position of the water relative to the center of mass of the BZN molecule. The change of the intermolecular bond length upon electronic excitation is larger than the distance change between the centers of mass of the two molecules. The changes can be explained by the structure change from S_0 [4] to S_1 [3] of the BZN

monomer. This means that the intermolecular bonding is only slightly affected by the electronic excitation.

For comparison the changes of the bond length upon electronic excitation in complexes between aromatics and rare gases are larger. E g. in benzene·Ar the Ar is located above the ring at a distance of 3.58 Å (3.52 Å) S_0 (S_1) [7]. The larger change of the bond distance after electronic excitation is caused by the influence of the π-electron excitation in the benzene ring on the van der Waals bonding due to the increasing polarizability in the electronically excited benzene. The in-plane side-on position of the water in BZNW is less influenced by the electronic $\pi\pi^*$-excitation localized in the ring. It is somewhat surprising that the attachment of the water does not change the structure of the electronically excited BZN. A still open question is in line with the proposed influence of the polar solvent water on the probability of charge transfer reactions. Further investigation of the vibrations in S_1 is needed in order to interpret the consequences of this result on the influence of the polar solvent water on the excited state leading to TICT or RICT [11, 12] states.

IV. Summary and Conclusion

In this work we presented highly resolved spectra of the BZNW complex. The virtue of the special combination of MW and high resolution UV results yields information on the structure of this cluster between an aromatic molecule and water not only in the S_0 ground state but also in the S_1 excited state and demonstrates the effect of electronic $\pi\pi^*$-excitation on the structure and on the intermolecular bonding.

The technique of high resolution mass-resolved UV spectroscopy is applied for the first time to small hydrogen-bonded clusters yielding species-selective information. The observed line broadening after clustering with the polar H_2O points to an influence of the polarity of the clustering partner on the linewidth. Further investigations will clarify this point.

A structure fit reveals that the water is located near the plane of the BZN molecule with one or two water hydrogens off the plane. For S_0 (S_1) the distance of the oxygen to the ortho hydrogen is r_0 = 2.477(4) Å (2.457(2) Å) and the angle to the ortho carbon-hydrogen bond 143.34(2)° (141.91(3)°). The measured structure changes of the cluster from S_0 to S_1 can be explained by the change of the structure of the BZN monomer itself. The position of the water relative to the ortho hydrogen is only slightly affected by the electronic excitation.

The MW investigation will be extended to more isotopomers to get a better determination of the six relative parameters for the water position and orientation.

Further high resolution UV measurements of intermolecular vibronic bands in S_1 are supposed to yield information on the potential surface of the mixed van der Waals and hydrogen-bonding potential.

Acknowledgement

Financial support from the Deutsche Forschungsgemeinschaft (Schwerpunktprogramm Molekulare Cluster) and the Fonds der Chemie is gratefully acknowledged by both groups. The Munich group thanks Dr. Robert Neuhauser for helpful discussions and Elke Guthaus, Michael Müller and Rainer Gerthner for their experimental support. The Kiel group thanks the colleagues for help and discussion. D. C. acknowledges an Alexander-von-Humboldt fellowship. V. S. thanks the microwave group of Prof. W. Stahl at the RWTH Aachen for their hospitality.

[1] T. Kobayashi, K. Honma, O. Kajimoto, and S. Tsuchiya, J. Chem. Phys. **86**, 1111 (1987).
[2] T. Kobayashi and O. Kajimoto, J. Chem. Phys. **86**, 1118 (1987).
[3] R. M. Helm, H.-P. Vogel, and H. J. Neusser, Chem. Phys. Lett. **270**, 285 (1997).
[4] U. Dahmen, W. Stahl, and H. Dreizler, Ber. Bunsenges. Phys. Chem **98**, 970 (1994).
[5] M. Araki, S. Sato, and K. Kimura, J. Phys. Chem. **100**, 10542 (1996).
[6] G. Berden, W. L. Meerts, M. Schmitt, and K. Kleinermanns, J. Chem. Phys **104**, 972 (1996).
[7] Th. Weber, A. von Bargen, E. Riedle, and H. J. Neusser, J. Chem. Phys. **92**, 90 (1990).
[8] A. Held and D. W. Pratt, J. Am. Chem. Soc. **115**, 9708 (1993).

[9] W. Rettig, Angew. Chem. Int. Ed. Engl. **25**, 971 (1986).
[10] Z. R. Grabowski, K. Rotkiewicz, A. Siemiarczuk, D. J. Cowley, and W. Baumann, Nuov. J. Chim. **3**, 443 (1979).
[11] A. L. Sobolewski and W. Domcke, Chem. Phys. Lett. **250**, 428 (1996).
[12] A. L. Sobolewski and W. Domcke, Chem. Phys. Lett. **259**, 119 (1996).
[13] R. A. Weersink and S. C. Wallace, J. Phys. Chem **98**, 10710 (1994).
[14] O. Kajimoto and S. Hayami, Chem. Phys. Lett. **177**, 219 (1991).
[15] B. D. Howells, J. McCombie, T. Frank Palmer, J. P. Simons, and A. Walters, J. Chem. Soc. Far. Trans. **88**, 2603 (1992).
[16] R. C. Weast and M. J. Astle, Handbook of Chemistry and Physics; CRC Press, Boca Raton 1979.
[17] V. Storm, H. Dreizler, D. Consalvo, J.-U. Grabow, and I. Merke, Rev. Sci. Instrum. **67**, 2714 (1996).
[18] U. Andresen, H. Dreizler, U. Kretschmer, W. Stahl, and C. Thomsen, Fresenius J. Anal. Chem. **349**, 272 (1994).
[19] J.-U. Grabow, W. Stahl, and H. Dreizler, Rev. Sci. Instrum. **67**, 4072 (1996).
[20] R. Sußmann, R. Neuhauser, and H. J. Neusser, Can. J. Phys. **72**, 1179 (1994).
[21] E. Riedle, R. Moder, and H. J. Neusser, Opt. Commun. **43**, 388 (1982).
[22] S. Gerstenkorn and P. Luc, Atlas du spectre d'absorption de la molecule d'Iode, Centre du National de la Recherche Scientifique; CNRS, Paris 1978.
[23] S. Gerstenkorn and P. Luc, Rev. Phys. Appl. **14**, 791 (1979).
[24] G. Herzberg, Electronic Spectra of Polyatomic Molecules; Van Nostrand, Princeton 1967, Chapt. II.3.
[25] R. N. Pribble and T. S. Zwier, Faraday Discuss. **97**, 229 (1994).
[26] U. Andresen, H. Dreizler, J.-Z. Grabow, and W. Stahl, Rev. Sci. Instrum. **61**, 3694 (1990).
[27] J. Casado, L. Nygaard, and G. O. Sørensen, J. Mol. Struct. **8**, 211 (1971).
[28] W. Gordy and L. R. Cook, Microwave Molecular Spectra; J. Wiley and Sons, New York 1984, Chapt. VII, VIII.
[29] Program by V. Typke, Ulm.
[30] loc. cit. [28], Chapt. IX.
[31] J. Gripp and H. Dreizler, Z. Naturforsch. **45 a**, 715 (1990).
[32] J. Gripp, PhD. Thesis, Kiel 1989.
[33] H. W. Kroto, Molecular Rotation Spectra; J. Wiley and Sons, London, 1975, Chapt. III.
[34] R. M. Helm, H.-P. Vogel, and H. J. Neusser (unpublished).
[35] U. Dahmen, Dipl. thesis, Kiel 1993.
[36] F. C. Lucia, P. Helminger, and W. Gordy, Phys. Rev. A **8**, 2785 (1973).
[37] M. Gerhards, M. Schmitt, K. Kleinermanns, and W. Stahl, J. Chem. Phys. **104**, 967 (1996).
[38] loc. cit. [28], Chapt. XIII.7, XIII.2.
[39] loc. cit. [28], Chapt. XIII.1, XIII.7.
[40] H. D. Rudolph, Struct. Chem. **2**, 581 (1991); Adv. Mol. Struct. Research **1**, 63 (1995).
[41] loc. cit. [28], Chapt. XIII.3.
[42] L. D. Landau and E. M. Lifschitz, Lehrbuch der theoretischen Physik I, Mechanik; Akademie-Verlag, Berlin 1976, Chapt. VI
[43] W. H. Press, S. A. Teukolsky, W. T. Vetterling, and B.P. Flannery, Numerical Recipes in C: The art of scientific computing; Cambridge University Press, Cambridge 1992, Chapt. X.
[44] B. P. van Eijck, J. Mol. Spectrosc. **53**, 246 (1974).
[45] B. P. van Eijck, J. Mol. Spectrosc. **91**, 348 (1982).